NASA/TM—2018-219906

Joint Strength Optimization and Damping Assessment of NiTi-Polymer Matrix Hybrid Composites

Tiffany S. Williams, Sandi G. Miller, Gary D. Roberts, James B. Min, and Bradley A. Lerch
Glenn Research Center, Cleveland, Ohio

Lee W. Kohlman
Langley Research Center, Hampton, Virginia

Paula J. Heimann, Linda S. McCorkle, and Daniel A. Scheiman
Ohio Aerospace Institute, Brook Park, Ohio

Caldwell McFadden
North Carolina Agricultural and Technical State University, Greensboro, North Carolina

August 2018

NASA STI Program . . . in Profile

Since its founding, NASA has been dedicated to the advancement of aeronautics and space science. The NASA Scientific and Technical Information (STI) Program plays a key part in helping NASA maintain this important role.

The NASA STI Program operates under the auspices of the Agency Chief Information Officer. It collects, organizes, provides for archiving, and disseminates NASA's STI. The NASA STI Program provides access to the NASA Technical Report Server—Registered (NTRS Reg) and NASA Technical Report Server—Public (NTRS) thus providing one of the largest collections of aeronautical and space science STI in the world. Results are published in both non-NASA channels and by NASA in the NASA STI Report Series, which includes the following report types:

- TECHNICAL PUBLICATION. Reports of completed research or a major significant phase of research that present the results of NASA programs and include extensive data or theoretical analysis. Includes compilations of significant scientific and technical data and information deemed to be of continuing reference value. NASA counter-part of peer-reviewed formal professional papers, but has less stringent limitations on manuscript length and extent of graphic presentations.

- TECHNICAL MEMORANDUM. Scientific and technical findings that are preliminary or of specialized interest, e.g., "quick-release" reports, working papers, and bibliographies that contain minimal annotation. Does not contain extensive analysis.

- CONTRACTOR REPORT. Scientific and technical findings by NASA-sponsored contractors and grantees.

- CONFERENCE PUBLICATION. Collected papers from scientific and technical conferences, symposia, seminars, or other meetings sponsored or co-sponsored by NASA.

- SPECIAL PUBLICATION. Scientific, technical, or historical information from NASA programs, projects, and missions, often concerned with subjects having substantial public interest.

- TECHNICAL TRANSLATION. English-language translations of foreign scientific and technical material pertinent to NASA's mission.

For more information about the NASA STI program, see the following:

- Access the NASA STI program home page at http://www.sti.nasa.gov

- E-mail your question to help@sti.nasa.gov

- Fax your question to the NASA STI Information Desk at 757-864-6500

- Telephone the NASA STI Information Desk at 757-864-9658

- Write to:
  NASA STI Program
  Mail Stop 148
  NASA Langley Research Center
  Hampton, VA 23681-2199

NASA/TM—2018-219906

Joint Strength Optimization and Damping Assessment of NiTi-Polymer Matrix Hybrid Composites

Tiffany S. Williams, Sandi G. Miller, Gary D. Roberts, James B. Min, and Bradley A. Lerch
Glenn Research Center, Cleveland, Ohio

Lee W. Kohlman
Langley Research Center, Hampton, Virginia

Paula J. Heimann, Linda S. McCorkle, and Daniel A. Scheiman
Ohio Aerospace Institute, Brook Park, Ohio

Caldwell McFadden
North Carolina Agricultural and Technical State University, Greensboro, North Carolina

National Aeronautics and
Space Administration

Glenn Research Center
Cleveland, Ohio 44135

August 2018

Acknowledgments

This work was supported by the NASA Advanced Air Transport Technology Project. The authors would like to acknowledge support from the Glenn Capstone Research Program between NASA Glenn Research Center and North Carolina A&T State University. The authors would also like to thank Drs. Santo Padula and Othmane Benefan for their valuable expertise on the behaviors of NiTi alloys and Dr. Euy-Sik Shin for his advice on lap shear testing.

This work was sponsored by the Advanced Air Vehicle Program at the NASA Glenn Research Center

Level of Review: This material has been technically reviewed by technical management.

Available from

NASA STI Program
Mail Stop 148
NASA Langley Research Center
Hampton, VA 23681-2199

National Technical Information Service
5285 Port Royal Road
Springfield, VA 22161
703-605-6000

This report is available in electronic form at http://www.sti.nasa.gov/ and http://ntrs.nasa.gov/

Joint Strength Optimization and Damping Assessment of NiTi-Polymer Matrix Hybrid Composites

Tiffany S. Williams, Sandi G. Miller, Gary D. Roberts, James B. Min, and Bradley A. Lerch
National Aeronautics and Space Administration
Glenn Research Center
Cleveland, Ohio 44135

Lee W. Kohlman
National Aeronautics and Space Administration
Langley Research Center
Hampton, Virginia 23681

Paula J. Heimann, Linda S. McCorkle, and Daniel A. Scheiman
Ohio Aerospace Institute
Brook Park, Ohio 44142

Caldwell McFadden
North Carolina Agricultural and Technical State University
Greensboro, North Carolina 27401

Summary

Approaches to optimize the adhesive joint strength between shape memory alloy ribbons and carbon fiber-reinforced epoxy composites were investigated for potential use as either an actuating structure or a dampening composite for structural applications. The interfacial bond strength between nickel-titanium (NiTi) and a polymer matrix composite (PMC) was measured by double lap shear testing as a function of NiTi surface treatment and adhesive material. The effect of NiTi surface treatment on damping was investigated using dynamic mechanical analysis. Lap shear data show that treating the surfaces of NiTi ribbons by light sandblasting and primer application increased the interfacial bond strength by 20 percent over the baseline composite structure. Lap shear data also reveal that out of three different film adhesives investigated, samples bonded with AF 191U and Hysol® 9696U display the highest adhesive joint strengths. Optical microscopy reveals that most samples failed by either cohesive failure within the adhesive or by adhesive failure at either the adhesive/PMC or NiTi/adhesive interface. Adhering NiTi to the PMC did not appear to negatively impact damping performance; however, a more thorough examination into NiTi's role on vibration damping should be investigated.

1.0 Introduction

NASA is interested in investigating unique designs and configurations of various materials to enhance aerodynamic efficiency. Developing morphing aircraft structures or structures with enhanced vibration damping performance are highly desirable to help improve aerodynamic efficiency, performance, and structural longevity. Shape memory alloys (SMAs) are well-known smart materials that can change shape by undergoing temperature-dependent phase transitions and may perform reliably under many actuation events. Those same phase transitions observed to take place in the SMAs could also be responsible for their damping performance.

Fan blades are large structures believed to have the most potential to impact engine performance if camber angles were adaptable in certain flight conditions (Refs. 1 and 2). Camber angle changes as small as 4° between takeoff and cruise are predicted to be effective at reducing fuel burn by as much as 0.5 to 1.5 percent (Ref. 2). Integration of SMAs, such as nickel-titanium (NiTi), with polymer matrix composites (PMCs) could be a viable option for advancing the development of lightweight morphing aircraft structures (Refs. 2 to 4).

Both SMAs and PMCs have been thoroughly investigated for various applications in aerospace, but as of now, a "smart" structure has not been implemented because of the complexity of typical behavior predicted in SMA-PMC hybrid composites (Ref. 5). Many studies have reported on the thermomechanical responses of SMA-PMC hybrid composites during processing and characterization to provide insight into SMA behavior during heating and PMC cure (Refs. 3 to 9), and it has been found that a key criterion for attaining sufficient actuation response in these hybrid composites is establishing and maintaining optimal interfacial adhesion between the SMA and PMC during repeat actuation events.

Metals and organic polymers are normally chemically incompatible and would more than likely yield poor, undesirable mechanical performance and actuation response if the surfaces of the SMAs and/or composites are not modified to enhance interfacial interactions (Refs. 10 and 11). Methods to improve compatibility or interfacial bond strength between metals and polymeric surfaces have been accomplished through sandblasting or hand-sanding to increase surface roughness and mechanical interlocking (Refs. 12 and 13), adding adhesion promoters (coupling agents) to increase interactions between thin surface oxides on the SMA and the reactive groups in the polymer (Refs. 10 and 14), treating with plasma (Ref. 15), chemical etching (Ref. 16), and applying film adhesives to bond the metal to the PMC (Refs. 16 and 17).

Fiber pullout, fiber pushout, and microbead techniques are well-known test methods that have been employed to evaluate the bond strength between fiber and matrix interfaces (Ref. 18). The methods share a similar concept: in all three methods, single fibers are embedded into a polymer matrix, and the amount of force that it takes to debond the fiber from the polymer is identified as the interfacial shear stress. The microbead, fiber pullout, and fiber pushout tests are more appropriate if single fibers or filaments are used. In fact, single fiber pullout tests are considered to be a widely accepted method to characterize NiTi wire/polymer interfaces (Refs. 10, 15, and 19 to 21). One disadvantage to measuring the interfacial shear strength of single fibers embedded in a matrix is that dozens of tests should be performed per sample in order to gather enough data that is representative of the composite in its entirety.

Another disadvantage when using bundles of single SMA wires as an actuator in a large SMA composite structure is that a significant number of SMA wires would have to be embedded into the PMC to achieve the desired deflection ranges, which may introduce limitations for this type of system to be implemented as a morphing aircraft structure. Shape memory alloy foils, ribbons, tapes, or sheets are alternative formats to SMA wires that can cover large surface areas and may be more effective actuators and dampeners than bundles of wires, if used in a large structure. Achieving sufficient bonding is essential if film adhesives are to be used to adhere larger material formats of SMAs to PMCs for structural applications (Ref. 22), but as of now, there is still a lack of systematic studies related to optimizing SMA-PMC joint strength and bond durability in these types of materials.

Both single and double lap shear are methods designed to provide some understanding about the strength of adhesive joints under shear loading (Ref. 23). Single lap shear testing is the most common and simplistic method to measure the adhesion strength of the joint, but this method is not suitable for all material types. The double lap shear design is commonly used to produce a symmetric joint to minimize out-of-plane normal stresses (Ref. 23). In this paper, the fabrication of SMA-PMC composites are described and the effects of substrate surface treatment and adhesive material on the joint strength of each composite are discussed according to double lap shear testing. Effects of NiTi surface treatment on the damping behavior of SMA-PMC coupons will also be discussed.

2.0 Experimental Procedures

2.1 NiTi and PMC Substrate Preparation and Double Lap Shear Specimen Fabrication

NiTi ribbons and the PMC host material were surface treated through physical and/or chemical processes to facilitate optimal bonding between the film adhesives and substrates. The following sections describe the procedures performed to clean and surface treat all substrates.

2.1.1 NiTi Preparation

NiTi ribbons ~0.006 in. (~0.15 mm) thick were cut to approximately 6.00 by 1.25 in. (152.40 by 31.75 mm) and cleaned by sonicating in hexane (Sigma Aldrich), isopropyl alcohol (Fisher Scientific), and ultrapure water sequentially for 20 min each. After cleaning, all NiTi strips were air dried and later grit blasted with 120-grit Al_2O_3 at 25 psi. The NiTi ribbons used in this study were not trained or processed in a way that the NiTi would remember a specific behavior. Figure 1 shows scanning electron microscopy (SEM) images of the effect of grit-blast pressure on surface roughness. Grit blasting at higher than 25 psi was avoided to prevent excessive surface roughness or pitting, which was observed in Figure 1(c), (e), and (f). Excessive roughness on the NiTi surface would have also eventually led to the formation of rich oxide layers on the NiTi surface, thus weakening the interfacial properties. After grit blasting, the as-received NiTi ribbons were rinsed clean in acetone and stored in a nitrogen-purged container prior to primer application and subsequent bonding to the PMC.

NiTi ribbons were primed by brushing with BR® 6747-1 primer (Cytec Engineered Materials Inc.) following grit blasting. The primer was applied by brushing (five cross-coats) and air drying the NiTi substrates at room temperature for 24 h. After 24 h, the primed NiTi ribbons were cured at 121 °C for 60 min to produce a scratch-resistant surface on the NiTi.

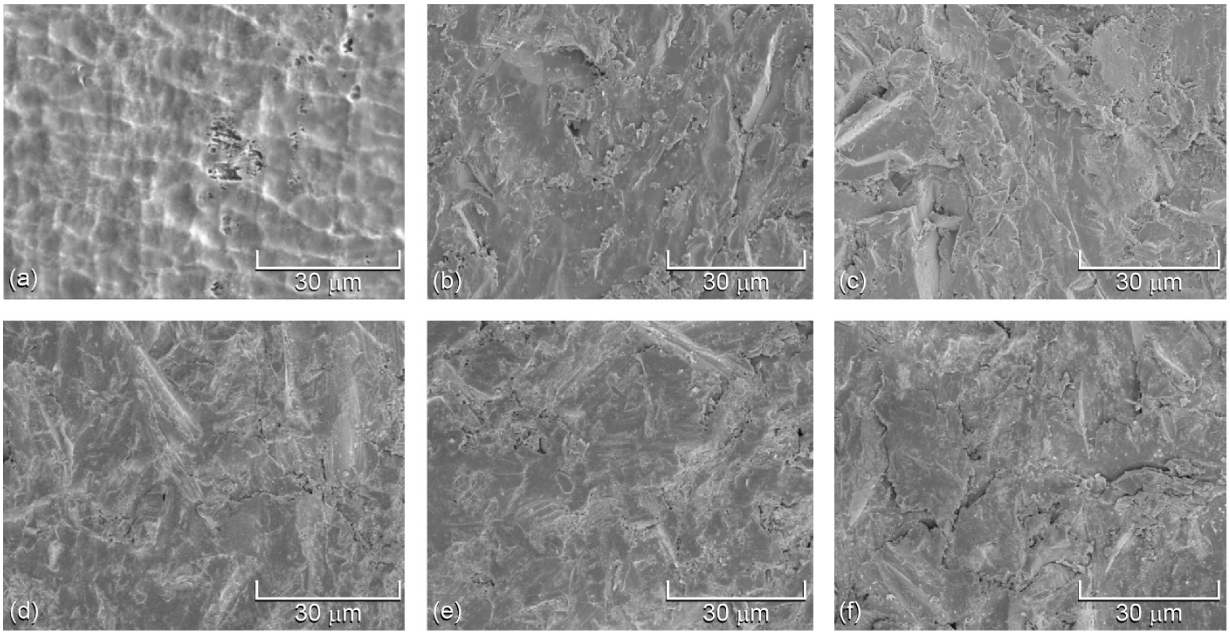

Figure 1.—Surface roughness of NiTi before and after grit blasting at different pressures. (a) As-received NiTi. (b) 15 psi. (c) 25 psi. (d) 40 psi. (e) 50 psi. (f) 60 psi.

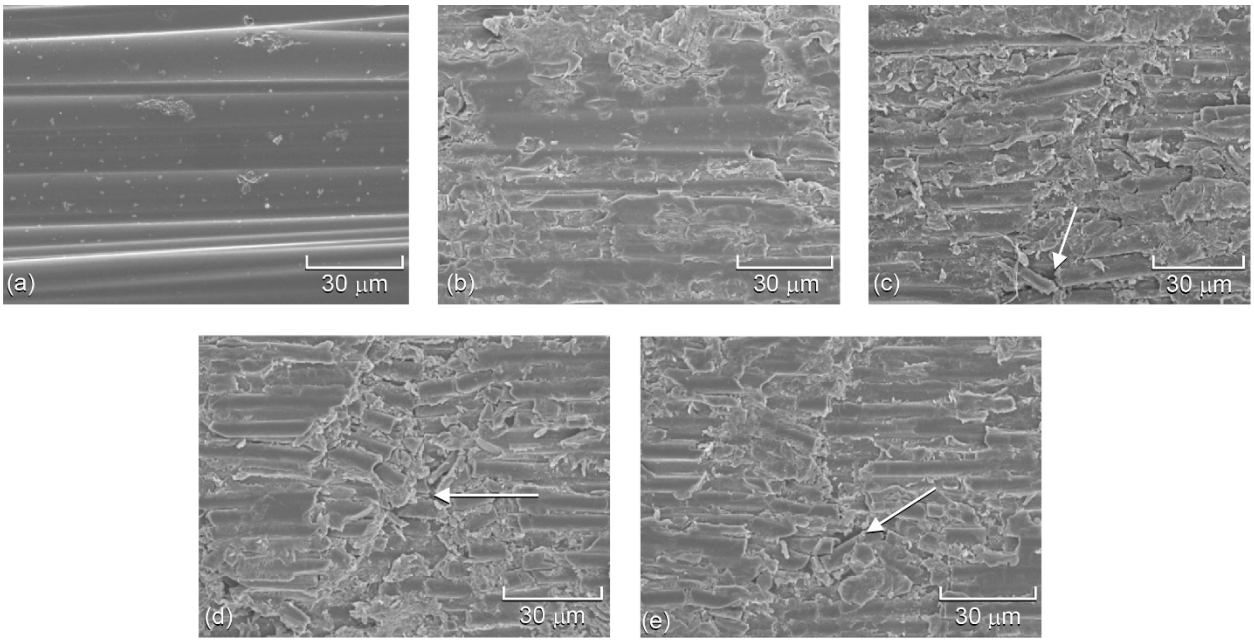

Figure 2.—Surface roughness of carbon fiber-reinforced epoxy composite (HexPly® 8552, Hexcel Corp.) before and after grit blasting at different pressures. (a) 0 psi. (b) 20 psi. (c) 40 psi. (d) 60 psi. (e) 80 psi.

2.1.2 Polymer Matrix Composite Fabrication

Carbon fiber-reinforced epoxy composite laminates that were used as the lap shear doublers and adherend panels were fabricated by laying up HexPly® 8552 (Hexcel Corporation) prepreg in a [0, 45, 90, –45] ply configuration and curing according to vendor-recommended procedures (Ref. 24). The PMC doublers consisted of 16 plies $[0, 45, 90, –45]_{2s}$, which corresponded to a thickness of ~0.08 in. (~2.0 mm), and each composite adherend comprised 32 plies $[0, 45, 90, –45]_{4s}$, which corresponded to a thickness of ~0.16 in. (~4.0 mm). The PMCs were cured in an autoclave where the samples were ramped to 225 °F (107 °C) and dwelled for 1 h, followed by ramping to 350 °F (177 °C) at 2 °F/min and dwelling for 2 h at 90 psi.

Composite surfaces in contact with the adhesive layer were lightly grit blasted with 120-grit Al_2O_3. Lightly grit blasting the PMC surfaces was carried out to remove residual release agents that may have been present on the composite surface after processing, thus avoiding reductions in the interfacial bond strength between the PMC and film adhesive. Light grit blasting may have also played a role in increasing surface roughness in the composite surface, which would contribute to better mechanical interlocking. Representative SEM images of the PMCs at various grit-blasting pressures are presented in Figure 2. The micrographs revealed that grit blasting higher than 40 psi (Figure 2(c)) led to fiber fragmentation and damage, which may be indicative of excessive resin removal and was therefore not recommended. Figure 2(b) shows that 20 psi was considered to be an ideal grit-blasting pressure for the PMC surfaces according to the SEM micrographs because no evidence of fiber fragmentation was observed.

2.1.3 Double Lap Shear Composite Panel Curing

A modified version of double lap shear test method (ASTM 3528–96, Ref. 25) was used to design the SMA-PMC test specimens to account for the SMA-PMC hybrid doubler as opposed to using a doubler made of a single material. The double butt joint configuration (Figure 3) was chosen to minimize stress concentrations in the SMA-PMC joints. Table I includes all SMA-PMC composites that were processed for double lap shear tests along with the surface treatment conditions. The specifications for all three adhesive materials are listed in Table II.

Each adhesive material was cured according to its vendor-recommended cure schedules as shown in Table III. All lap shear master panels were fabricated by secondary bonding the SMAs to PMCs with a film adhesive. Co-curing the SMA ribbons with the PMCs was not attempted as an effort to maintain consistency, because the optimum cure profiles of each film adhesive were all different from the PMC material. Dimensions of the master panels for double lap shear characterization were measured to be approximately 8.6 by 6.1 by 0.3 in. (~219 by 154.6 by 8.3 mm). Five smaller specimens were cut from each master panel to dimensions of approximately 8.6 by 1.0 by 0.3 in. (219 by 25.4 by 8.3 mm) as illustrated in Figure 3. The overlap region of each doubler was approximately 1 by 1 in. (25.4 by 25.4 mm).

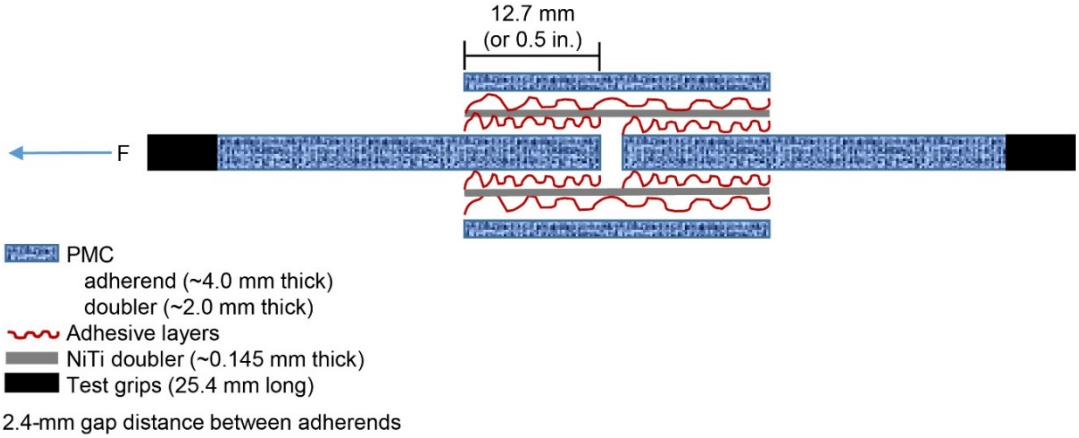

Figure 3.—NiTi-PMC (polymer matrix composite) double butt joint geometry used for lap shear specimens.

TABLE I.—NiTi-PMC (POLYMER MATRIX COMPOSITE) SYSTEMS STUDIED FOR ADHESIVE JOINT STRENGTH EVALUATION

Adhesive[a]		
AF 191U[b]	FM® 377U[c]	Hysol® 9696U[d]
NiTi (sandblasted, primed) + PMC (sandblasted)	NiTi (sandblasted, primed) + PMC (sandblasted)	1. PMC control (sandblasted), No NiTi 2. NiTi (no primer) + PMC (sandblasted) 3. NiTi (sandblasted, primed) + PMC (sandblasted)

[a]U indicates scrim: unsupported format.
[b]3M™ Scotch-Weld™ Structural Adhesive Film AF 191U, 3M Company.
[c]Cytec Engineered Materials Inc.
[d]LOCTITE® EA 9696 AERO, Henkel Corporation.

TABLE II.—ADHESIVE FILM SPECIFICATIONS

Specification	Adhesive[a]		
	AF 191U[b]	FM® 377U[c]	Hysol® 9696U[d]
Nominal weight, psf (gsm)	0.015 (73)	0.055 (269)	0.015 (73)
Nominal thickness, in. (mm)	0.0025 (0.065)	0.005 (0.13)	

[a]U indicates scrim: unsupported format.
[b]3M™ Scotch-Weld™ Structural Adhesive Film AF 191U, 3M Company.
[c]Cytec Engineered Materials Inc.
[d]LOCTITE® EA 9696 AERO, Henkel Corporation.

TABLE III.—ADHESIVE FILM CURE SCHEDULES

Adhesive[a]	AF 191U[b]	FM® 377U[c]	Hysol® 9696U[d]
Cure cycle	4 to 5 °F/min (2 to 3 °C/min) ramp to 350° F (177 °C), 45 psi (0.31 MPa). 60-min dwell at 350 °F (177 °C)	3.0 to 3.2 °F/min (~1.7 °C/min) ramp to 350 °F (177 °C), 40 ± 5 psi (0.28 ± 0.03 MPa). 90-min dwell at 350 °F (177 °C)	3.6 °F/min (2.0 °C/min) ramp to 250 °F (121 °C), 45 psi (0.31 MPa). 90-min dwell at 250 °F (121°C)

[a]U indicates scrim: unsupported format.
[b]3M™ Scotch-Weld™ Structural Adhesive Film AF 191U, 3M Company.
[c]Cytec Engineered Materials Inc.
[d]LOCTITE® EA 9696 AERO, Henkel Corporation.

2.1.4 SMA-PMC Damping Specimen Preparation

SMA-PMC hybrid composites for damping characterization were prepared by cutting ~0.18-in.- (~4.5-mm-) thick PMC specimens to ~1.0 by 0.3 in. (~25.0 by 8.5 mm) and adhering the NiTi foil to the host PMC via secondary bonding. The film adhesive that displayed the most optimal adhesion characteristics according to double lap shear analysis was selected for the NiTi-PMC damping study. The storage modulus (E'), loss modulus (E''), and damping factor ($\tan\delta$) of each sample were evaluated to determine the effects of surface treatment on NiTi's damping ability.

2.2 Characterization Methods

Microscopy was used to image the surface and bond failure of the substrate and lap shear test specimens, respectively. Double lap shear testing was performed to measure the bond strength as a function of adhesive material. Thermal analysis was used to identify the temperature-dependent phase transitions of NiTi, decomposition profiles of the film adhesives, and the damping capacity of the NiTi-PMC hybrid specimens.

2.2.1 Substrate Surface Imaging

A Hitachi S4700 scanning electron microscope was used to examine the surface quality of NiTi and IM7/8552 composites after grit blasting. Operating voltages between 6 and 8 keV were used.

2.2.2 Phase Transition Identification in NiTi

Differential scanning calorimetry (DSC) experiments were carried out to identify the temperature-dependent phase transitions in the NiTi foil. Calorimetry experiments were carried out using a TA Instruments Q1000 DSC. The average NiTi sample mass was ~47.5 mg. NiTi strips were cleaned, cut, and placed in aluminum DSC pans and covered with lids. All samples were equilibrated at –65 °C and heated to 180 °C at a rate of 5 °C/min. Samples were cooled back down to –65 °C and then heated again to 180 °C at 5 °C/min before cooling back to room temperature. DSC data were analyzed using TA Instruments Universal Analysis software.

2.2.3 Thermal Stability of Film Adhesives

Thermogravimetric analysis (TGA) was carried out using a TA Instruments Q500 Thermogravimetric Analyzer to determine the thermal stabilities of the uncured AF 191U, FM® 377U, and Hysol® 9696U film adhesives. Three specimens of each were tested. All samples were ramped to 900 °C at a rate of 10 °C/min under nitrogen. TGA data were analyzed using TA Instruments Universal Analysis software.

2.2.4 SMA-PMC Bond Strength Evaluation

Double lap shear tests were performed to measure the bond strength between treated NiTi, the epoxy film adhesive, and IM7/8552 PMCs. The tests were carried out using an MTS Testing Machine with a 22-kN load cell. The samples were mounted in tensile mode and pulled at a displacement rate of 2.0 in./min. Five specimens were tested for each material system. All tests were performed at room temperature. The interfacial shear stress (σ) was calculated by Equation (1), where the shear stress is defined as one-half of the applied tensile force (F), divided by the area of contact between one doubler and one adherend:

$$\sigma = \frac{F/2}{0.5 \text{ in. contact area}} = F \tag{1}$$

2.2.5 Posttest Analysis of SMA-PMC Surfaces

Following double lap shear testing, interfacial failure behaviors of the SMA-PMC hybrid composites were examined using a Nikon SMZ1270 stereo-optical microscope with NIS Elements D version 4.50 Imaging Software.

2.2.6 Dynamic Mechanical Analysis (DMA)

The thermomechanical properties of NiTi-PMC hybrid composites were measured by DMA. DMA was used primarily as a screening tool to determine the effect of NiTi on the thermomechanical properties of the SMA-PMC hybrid composites and the effect of NiTi surface modification on tan δ, E'', and E'. DMA tests were carried out using a TA Instruments Q800 Dynamic Mechanical Analyzer under single cantilever mode. TA Instruments Universal Analysis software was used to analyze the data. The damping factor was measured by performing a temperature ramp from 40 to 350 °C at 5 °C/min. A frequency of 1 Hz was used for standard temperature ramp tests.

3.0 Results and Discussion

3.1 Thermal Transitions in As-Received NiTi

Figure 4 represents the DSC thermogram of the as-received NiTi foil. Figure 4 illustrates that an endotherm appeared near 94 °C during the first heat ramp from –65 to 180 °C and is an indication of the martensite-to-austenite phase transition in NiTi. Two exotherms appeared near ~61 and 55 °C during the first cool cycle (from 180 to –65 °C) and captured the NiTi austenite-to-martensite phase transformation. The appearance of exothermic doublet peaks could be an indication of the "R-phase," the intermediate monoclinic martensite phase in NiTi. This doublet may also indicate inhomogeneity in the NiTi foil. The endothermic peak signifying the martensite-to-austenite transition decreased from ~94 to ~92 °C during the second heat cycle. The exothermic peaks illustrating the austenite-to-martensite transition remained fairly consistent to the transition temperatures observed during the first cool cycle.

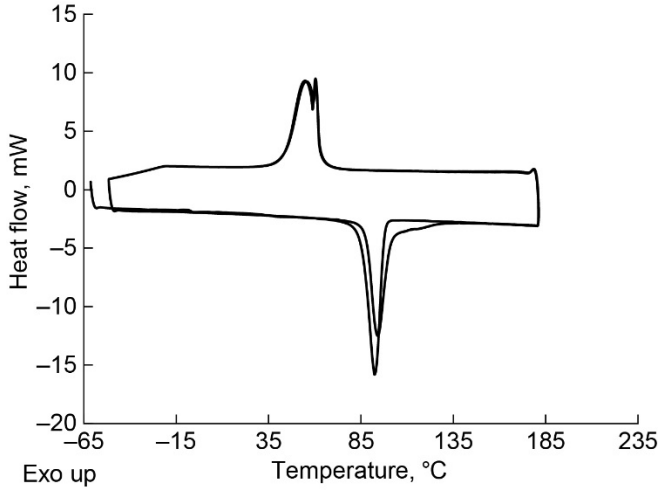

Figure 4.—Differential scanning calorimetry (DSC) thermogram illustrating phase transitions in as-received NiTi foil.

3.2 Thermal Stability of Epoxy Film Adhesives

TGA data presented in Figure 5 show the thermal stabilities for AF 191U, FM® 377U, and Hysol® 9696U epoxy film adhesives. Understanding the thermal stability between 90 and 100 °C was important, as this temperature range corresponded to phase transitions in NiTi and would confirm the ability of the film adhesive material to withstand continuous SMA actuation events near this temperature range. Figure 5 shows that all three film adhesives were fairly stable at 100 °C and indicates that all film adhesives investigated in this study would be suitable for applications where actuation would take place, near 100 °C. Table IV includes the onset decomposition temperatures (T_d) of all three film adhesives. Table IV reveals that the onset T_d of Hysol® 9696U at ~373 °C appeared to be the highest, because it possesses the broadest decomposition transition range of all three film adhesives.

3.3 Bond Strength Evaluation of SMA-PMC Composites

Double lap shear testing was performed on the baseline PMC, the SMA-PMC with primer applied to the NiTi, and an SMA-PMC with no primer applied to the NiTi. All samples were bonded with Hysol® 9696U adhesive for the NiTi surface treatment assessment. Table V illustrates that the PMC-to-PMC joint displays the lowest adhesive bond strength out of all samples with an average of ~4290 psi. No significant change in bond strength was observed when the NiTi without primer was integrated into the double lap shear design. Application of primer on the NiTi surfaces increased the bond strength by 20 percent (approx. 5316 psi) compared to the SMA-PMC sample without primer. The data highlights improved interfacial bond strength between the SMA and PMC through surface preparation through primer application and light sandblasting. It should be noted that in most reports, the bond strength between primers and adhesives have been predominantly carried out using aluminum substrates and not NiTi, so the effectiveness of the primer applied to NiTi alloys were unknown prior to this study.

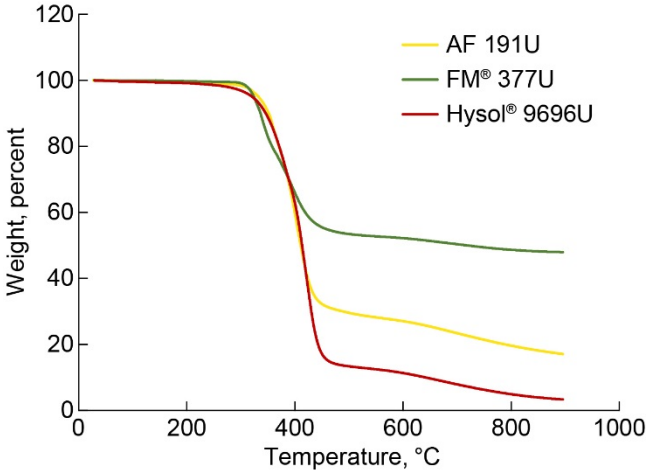

Figure 5.—Thermogravimetric analysis data for AF 191 (3M Company), FM® 377 (Cytec Engineered Materials Inc.), and Hysol® 9696 (Henkel Corporation) film adhesives.

TABLE IV.—ONSET DECOMPOSITION TEMPERATURE (T_d) FOR FILM ADHESIVES

[Error represents 1 standard deviation from three specimens.]

Adhesive[a]	AF 191U[b]	FM® 377U[c]	Hysol® 9696U[d]
Average onset T_d, °C	355.8±1.6	317.9±1.1	373.4±1.4

[a]U indicates scrim: unsupported format.
[b]3M™ Scotch-Weld™ Structural Adhesive Film AF 191U, 3M Company.
[c]Cytec Engineered Materials Inc.
[d]LOCTITE® EA 9696 AERO, Henkel Corporation.

Following double lap shear testing, all specimens were imaged with a stereo-optical microscope to evaluate the fracture surfaces. The imaged region of the test coupon is shown in Figure 6. Figure 7(a) shows a section of the PMC adherend bonded to the PMC doubler. Residual Hysol® 9696U adhesive was observed on both the adherends and doublers, with most samples overall still showing sufficient adhesive coverage on the PMC substrates. Figure 7(b) shows a section of the SMA-PMC with primer applied to the NiTi-PMC hybrid doubler. As can be seen from the micrograph, the Hysol® 9696U epoxy also appeared to adhere well to the primed NiTi-PMC doubler. Figure 7(c) shows the SMA-PMC with no primer applied to the NiTi component of the NiTi-PMC doubler. The micrograph shows that the film adhesive had better uniformity in the primed NiTi-PMC coupons compared to the NiTi-PMC coupons without primer, thus serving as another indication of the role of the primer enhancing the interfacial bond strength between NiTi and the PMC.

TABLE V.—BOND STRENGTH OF NiTi-PMC[a] HYBRID SPECIMENS USING HYSOL® 9696[b] ADHESIVE
[Error represents one standard deviation from five specimens.]

	PMC-to-PMC control (no NiTi)	PMC-to-NiTi (no primer)	PMC-to-NiTi (primed)
Double lap shear strength, psi	4290.4±698.6	4417.4±262.7	5316.7±232.1
Failure location	Cohesive failure within adhesive and some substrate failure	Cohesive failure within adhesive	Cohesive failure within adhesive

[a]PMC is polymer matrix composite.
[a]LOCTITE® EA 9696 AERO, Henkel Corporation.

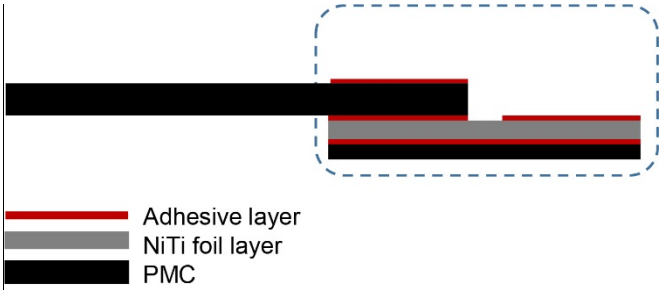

Figure 6.—Representative section of NiTi-PMC (polymer matrix composite) double lap shear sample imaged for optical microscopy after failure. Residual adhesive remained on NiTi surface for most specimens after double lap shear failure.

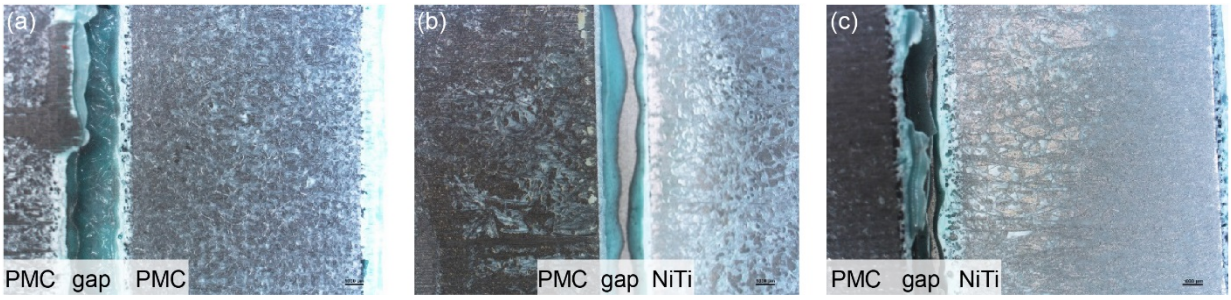

Figure 7.—Optical microscopy images of Hysol® 9696U bonded to NiTi shape memory alloy (SMA) and polymer matrix composite (PMC) adherends. Left side of each micrograph shows one side of PMC adherend. Right side of micrograph shows bottom half of doubler. “Gap” refers to 2.4-mm gap between adherends (see Figure 3). (a) PMC. (b) SMA-PMC with primer. (c) SMA-PMC without primer.

Both cohesive failure within the adhesive and adhesive failure (either at the PMC or NiTi substrate interfaces) were commonly observed failure modes in double lap shear coupons. However, because the samples in this study were made of a two-part SMA-PMC doubler system, variations in failure were complex in some instances. Figure 8 illustrates the most common types of failure observed in the PMC and SMA-PMC samples: adhesive failure at the PMC interface and cohesive failure within the adhesive layer.

More thorough descriptions of each specimen's failure behavior bonded with the Hysol® 9696U adhesive are shown in Table VI. Not all specimens followed the failure modes shown in Figure 8 because the adherends and doublers in some double lap shear specimens remained intact after failure. This behavior was mostly observed in the SMA-PMC specimens without primer. The majority of primed SMA-PMC coupons failed by cohesive failure through the adhesive layer, which is indicative of ideal bonding.

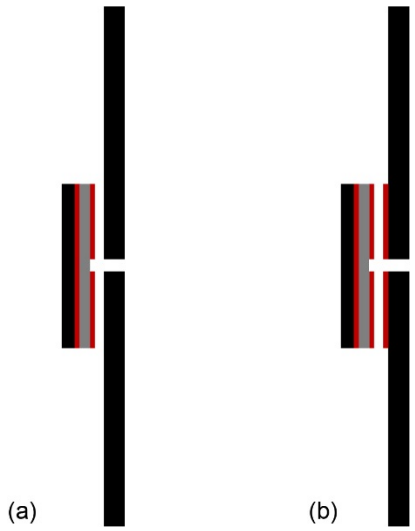

Figure 8.—Common failure modes observed in double lap shear NiTi-PMC specimens.
(a) Adhesive failure at PMC interface.
(b) Cohesive failure within adhesive.

TABLE VI.—FAILURE MODES OF NiTi-PMC HYBRID DOUBLE LAP SHEAR TEST SPECIMENS WITH HYSOL® 9696[a] FILM ADHESIVE

	PMC only	NiTi with surface primer	NiTi without primer
Specimen A	Cohesive failure within adhesive	Cohesive failure within adhesive	Cohesive failure within adhesive
Specimen B	Mixture of adhesive and substrate failure	Cohesive failure within adhesive	Cohesive failure within adhesive
Specimen C	Mostly cohesive within adhesive; minor substrate failure	Cohesive failure within adhesive	Cohesive failure within adhesive
Specimen D	Mostly cohesive failure within adhesive; minimal substrate failure	Cohesive failure within adhesive; minimal PMC substrate failure	Indiscernible: specimen intact after failure was detected
Specimen E	Mostly cohesive failure within adhesive; minimal substrate failure	Cohesive failure within adhesive	Indiscernible: specimen intact

[a]LOCTITE® EA 9696 AERO, Henkel Corporation.

3.4 Effect of Adhesive Material on Bond Strength in SMA-PMC Hybrid Specimens

Selection of the most promising film adhesive to bond to the primed NiTi-IM7/8552 composite was determined by measuring the interfacial bond strength of the SMA-PMC double lap shear samples with AF 191U, FM® 377U, and Hysol® 9696U film adhesives. The BR® 6747-1 primer was recommended by the vendor to be used specifically with the Cytec FM® 377U film adhesive; however, the same primer was also used for the other two adhesive materials in this study in an effort to maintain consistency in evaluating the primer's influence on NiTi substrates.

Table VII summarizes the interfacial bond strength of all three adhesive candidates used to bond the NiTi to all PMC laminates. The data indicate that the interfacial bond strength of the Hysol® 9696U was nearly 20 percent higher than that of FM® 377U, and about 13 percent higher than that of AF 191U.

Following double lap shear testing, the failure modes of all three adhesive candidates were investigated by optical microscopy. Figure 9 shows fracture surfaces of the double lap shear specimens similar to the section depicted in Figure 7. The AF 191U (Figure 9(a)) composite shows good adhesive contact with the NiTi after lap shear testing, but in some cases partial failure of the PMC adherend was observed. Bonding NiTi-PMC hybrid composites using the FM® 377U adhesive (Figure 9(b)) appears less than optimal, as mostly adhesive failure on either the PMC adherends or the primed NiTi surfaces was observed. Composites bonded with the Hysol® 9696U (Figure 9(c)) overall had the best coverage and adhesion to both the PMC adherend (left side of image) and the primed NiTi surface (right side of image).

Additional details regarding the SMA-PMC failure modes can be found in Table VIII. Table VIII shows that most Hysol® 9696U samples failed by cohesive failure within the adhesive layer, which is preferred. Many specimens bonded with FM® 377U displayed catastrophic adhesive failure, with either one or both doublers snapping off completely during testing. Quite a few AF 191U specimens also had either one or both doublers snap off during testing. No doublers fell off during testing of samples with the Hysol® 9696U adhesive.

TABLE VII.—INTERFACIAL BONDING OF NiTi-PMC HYBRID COMPOSITES WITH PRIMED NiTi RIBBONS AND DIFFERENT ADHESIVES
[Error bars represent 1 standard deviation as determined from five specimens.]

	Adhesive[a]		
	AF 191U[b]	FM® 377U[c]	Hysol® 9696U[d]
Double lap shear strength, psi	4674.5±698.6	4428.1±221.8	5316.7±232.1

[a]U indicates scrim: unsupported format.
[b]3M™ Scotch-Weld™ Structural Adhesive Film AF 191U, 3M Company.
[c]Cytec Engineered Materials Inc.
[d]LOCTITE® EA 9696 AERO, Henkel Corporation.

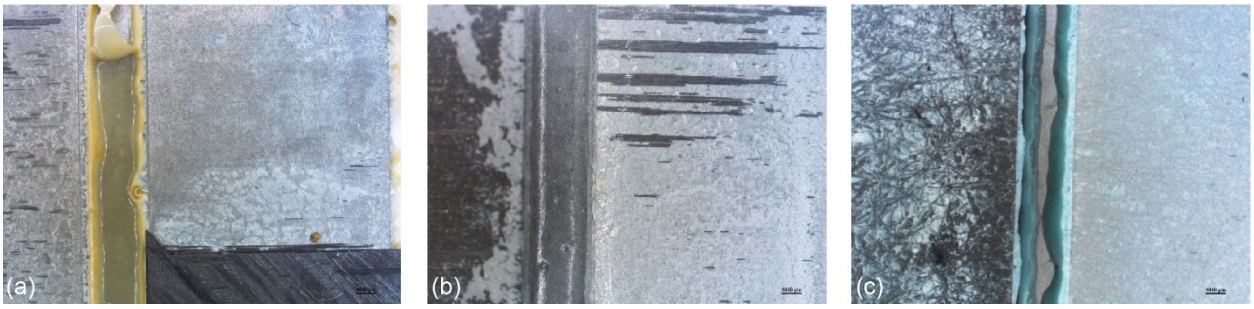

Figure 9.—Optical micrographs of fracture surfaces of NiTi-PMC laminates with different adhesives. Left side of each micrograph shows one side of PMC adherend. Right side of micrograph shows NiTi portion of doubler. Black areas represent layers of PMC. (a) AF 191U (3M Company). (b) FM® 377U (Cytec Engineered Materials Inc.). (c) Hysol 9696U (Henkel Corporation).

TABLE VIII.—FRACTURE MORPHOLOGY OF NiTi-PMC HYBRID COMPOSITES FROM DOUBLE LAP SHEAR POSTTESTS WITH DIFFERENT ADHESIVES

Specimen	Adhesive[a]		
	AF 191U[b]	FM® 377U[c]	Hysol® 9696U[d]
A	Indiscernible: specimen intact	Two doublers off Mostly adhesive failure at PMC interface	Cohesive failure within adhesive
B	One doubler off Mixture of PMC substrate and cohesive failure within adhesive	One doubler off Mostly adhesive failure at PMC interface	Cohesive failure within adhesive
C	One doubler off Mostly adhesive failure at PMC interface	Two doublers off Partial adhesive failure at PMC interface Partial PMC substrate failure	Cohesive failure within adhesive
D	Two doublers off Some cohesive failure within adhesive	One doubler off Partial cohesive failure within adhesive Minimal PMC substrate failure	Cohesive failure within adhesive Minimal PMC substrate failure
E	One doubler off Some cohesive failure within adhesive layer	One doubler off Partial PMC substrate failure Mostly adhesive failure at PMC interface	Cohesive failure within adhesive

[a]U indicates scrim: unsupported format.
[b]3M™ Scotch-Weld™ Structural Adhesive Film AF 191U, 3M Company.
[c]Cytec Engineered Materials Inc.
[d]LOCTITE® EA 9696 AERO, Henkel Corporation.

3.5 Effect of NiTi Surface Treatment on Damping Performance in NiTi-PMC Hybrid Composites

In addition to investigating the use of NiTi-PMC hybrid composites for morphing applications, these composites could also be used as a structure to dampen vibrations since NiTi is known to possess good damping properties (Ref. 26). Integrating NiTi with PMCs into locations of a structure that would be exposed to high levels of vibrational energy could be advantageous to save on mass compared to implementation of an all-metal structure. To investigate NiTi's effects on damping in the SMA-PMC hybrid composites, samples were prepared similarly to those in the double lap shear test study. Hysol® 9696 film adhesive was the only film adhesive material used for the damping study. The effects of NiTi surface treatment on damping behavior of the NiTi-PMC hybrid specimens were evaluated using DMA.

Prior to characterizing the thermomechanical properties of the SMA-PMC hybrid composites, the thermomechanical properties of each PMC component were characterized. Figure 10(a) shows the storage modulus (E') for the PMC, and the loss modulus (E'') and damping factor ($\tan\delta$) of the PMC are shown in Figure 10(b). Figure 10(a) shows that E' for the PMC is approximately 6900 MPa at 40 °C. A slope change beginning near 165 °C is indicative of the onset glass-transition temperature (T_g). Figure 10(b) shows that the E'' and $\tan\delta$ peak maxima appear at about 178 °C. Both E'' and $\tan\delta$ peaks are also representative of the PMC's T_g. Below the onset T_g, the $\tan\delta$ for PMC maintained a nearly constant value of about 0.045.

Figure 11 shows the effects of the addition of the NiTi layer and NiTi surface treatment on the storage modulus of NiTi-PMC laminates. As illustrated in Figure 11, there was only one transition for the neat PMC. When NiTi was adhered to the PMC substrate (also Figure 11), a small transition was observed near 100 °C, which was believed to correspond to the NiTi phase transition. It is near this temperature where the NiTi is believed to introduce damping. A slope change near 125 °C also appeared, which was more than likely caused by a transition within the Hysol® 9696 film adhesive. The final slope change began near 170 °C in the NiTi-PMC hybrid composites and was caused by a transition taking place in the matrix of the IM7/8552 PMC. The slope change in the NiTi-PMC hybrid composites shifted to about 5 °C higher compared to the PMC material without NiTi. There was no significant difference in the change in E' when NiTi was adhered to the composite. The E' in rubbery plateau regions (above ~180 °C) for all NiTi-containing specimens were higher than that of the rubbery plateau region of the PMC.

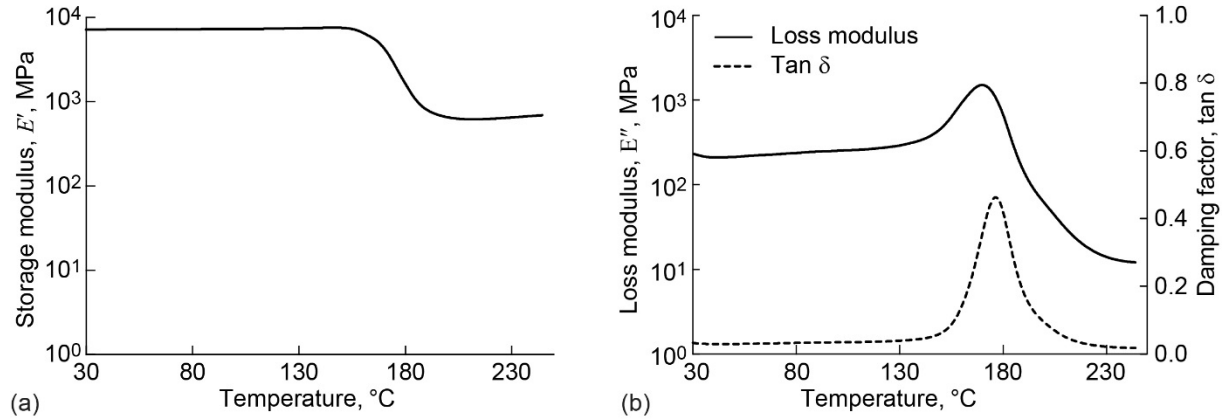

Figure 10.—Carbon fiber-reinforced epoxy thermomechanical properties. (a) Storage modulus E'. (b) Loss modulus E'' and damping factor tan δ.

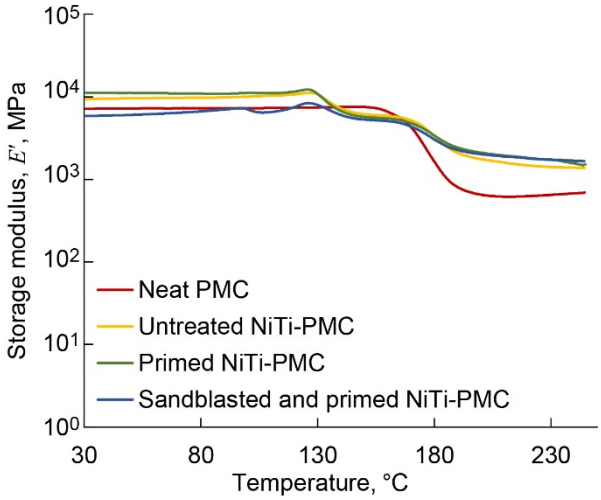

Figure 11.—Effect of NiTi surface treatment on storage modulus E' of NiTi-PMC hybrid specimens.

Figure 12 shows the effects of NiTi and NiTi surface treatment on the loss modulus E'' and tan δ, or damping factor, of the NiTi-PMC samples. The small peak appearing near 100 °C was more prominent overall in the loss modulus data (Figure 12(a)) than in the storage modulus data presented in Figure 11. The peak at 100 °C was more than likely attributed to the phase transition from the martensite to the austenite phase in NiTi. A larger peak appeared near 130 °C, which represented the T_g of the film adhesive, and was followed by the appearance of another large peak at approximately 178 °C, which was representative of the T_g of the epoxy in the PMC. Again, the peaks corresponding to the T_g of the PMC matrix in Figure 12 were observed to shift to higher temperatures after NiTi was bonded to the PMC.

The tan δ is calculated from the ratio of the loss modulus to the storage modulus (E''/E'). E'' typically represents the amount of irrecoverable energy in a material or the material's viscous response. E' is known as the component that depicts the material's recoverable energy or elastic response. Materials with lower tan δ values approaching 0 is an indication of the material displaying stiffer (more elastic) behavior, whereas higher tan δ values approaching 1 typically indicate that the material has better damping properties. Figure 12(a) shows that almost all of the NiTi-PMC hybrid specimens had higher loss modulus values than the neat PMC, which would suggest that NiTi-containing samples have a higher damping capacity than the PMC. Figure 12(b) shows that other than the appearance of peaks near 130 and 177 °C caused by the film adhesive and PMC matrix, respectively, there was very little change in the tan δ between the samples. The tan δ peak at the PMC's T_g was noticeably higher than that of the NiTi-PMC hybrid specimens', and may have been suppressed by the NiTi adhered to the PMC surface. Observing the storage modulus behaviors of NiTi-PMC specimens in Figure 11 and Figure 12 could suggest that the NiTi-PMC has higher damping attributes without compromising overall composite stiffness.

Table IX lists the thermomechanical properties of the NiTi-PMC hybrid specimens at room temperature (RT) and 100 °C. As mentioned earlier, evaluating the thermomechanical properties near 100 °C was important because the NiTi undergoes a phase transition near 100 °C. Unlike polymers, temperature-dependent transitions in SMAs should not correspond to irreversible losses in mechanical strength. For this reason, repetitious thermal cycling to temperatures exceeding the phase transition temperature of the SMA is not believed to negatively impact material performance.

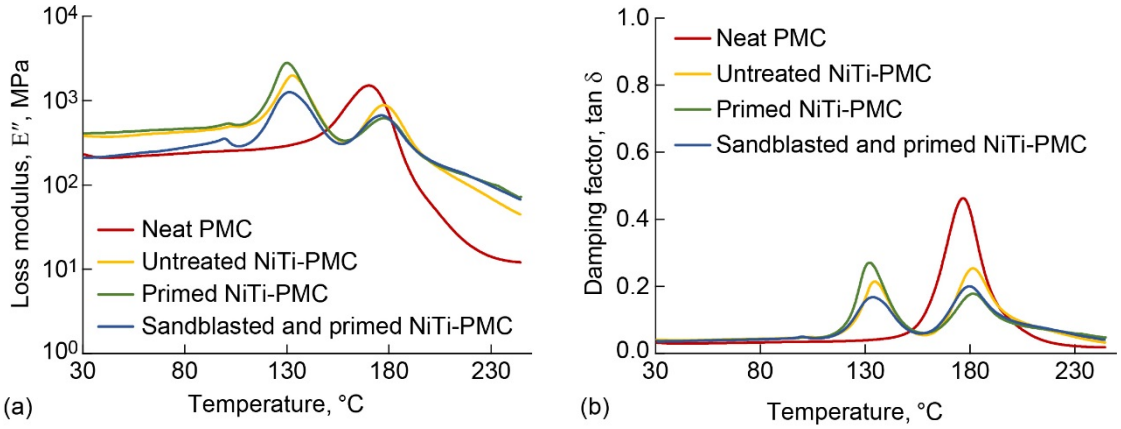

Figure 12.—Effect of NiTi surface treatment on NiTi-PMC hybrid specimens. (a) Loss modulus E''. (b) Damping factor tan δ.

TABLE IX.—STORAGE MODULUS (E'), LOSS MODULUS (E''), AND DAMPING FACTOR (tan δ) OF POLYMER MATRIX COMPOSITES (PMCs) AND SURFACE-TREATED NiTi-PMC HYBRID SPECIMENS

[Error bars represent 1 standard deviation as determined from at least three specimens.]

Property		PMC	Untreated NiTi-PMC	Primed PMC	Sandblasted + primed NiTi-PMC
E', GPa	Room temperature	6.90±0.51	8.89±0.99	11.92±2.90	5.32±0.79
	100 °C	6.99±0.52	9.11±1.27	12.29±2.73	6.07±0.78
E'', MPa	Room temperature	309±165	330±82	525±205	204±37
	100 °C	354±154	467±130	715±225	351±35
Tan δ	Room temperature	0.0444±0.0220	0.0369±0.00535	0.0468±0.00412	0.0384±0.00331
	100 °C	0.0502±0.0201	0.0506±0.00942	0.0577±0.00861	0.0579±0.0114

Table IX shows that in all cases, with and without the NiTi, the E', E'', and tan δ values were either the same or higher near 100 °C than at RT. However, samples containing the NiTi strip showed more significant changes between the RT and 100 °C range than the PMC material alone. The film adhesive could have also played a role in the more prominent thermomechanical property changes, but the change in interfacial bond strength between the NiTi and PMC as a function of NiTi surface treatment is believed to be the primary contributor to the changes in thermomechanical properties within this temperature range.

The increase in E' between room temperature and 100 °C in a given sample for the PMC and NiTi-PMC hybrids was not significant. However, the increase in E'' between RT and 100 °C was about 14 percent higher for the PMC and 41, 71, and 36 percent higher in the untreated NiTi, the primed NiTi, and the sandblasted and primed NiTi-PMC specimens, respectively. It is unclear if these changes are due to residual stresses from the phase transitions in the NiTi or if the changes imply that the SMA-PMC coupons' viscous response was enhanced as a function of NiTi surface treatment at 100 °C.

According to Table IX, the tan δ on average was highest for the PMC than the NiTi-PMC samples at room temperature. The damping factor for the PMC was approximately 13 percent higher at 100 °C compared to at room temperature. When NiTi was introduced, the change in the damping factor between room temperature and 100 °C was about 37 percent higher for the untreated NiTi, 50 percent higher for the primed NiTi, and 23 percent higher for the sandblasted + primed NiTi. This again suggests that there are some changes in the damping response which may be influenced by either residual stresses due to the SMA phase transitions and/or changes in interfacial bonding as a result of NiTi surface treatment. Because the loss moduli were higher in NiTi-containing laminates as a function of NiTi surface treatment, the damping factor was lower than the PMC. As a result, the tan δ data for NiTi-PMC samples did not appear to show a positive influence on improving damping according to DMA.

An added benefit to considering NiTi and other SMAs for aerospace applications is that these alloys can be tailored through processing or pre-straining, which could lead to enhancements in recovery strain and vibration damping (Ref. 26). Further analysis into the role of the NiTi on damping response in NiTi-PMC specimens will have to be carried out, because DMA alone is not the best method to evaluate NiTi's effectiveness on damping.

4.0 Conclusions

The effects of the adhesive material and nickel-titanium (NiTi) surface treatment on the interfacial bond strength in hybrid composites of shape memory alloy (SMA) and polymer matrix composite (PMC) were investigated. Application of an epoxy primer to surface roughened NiTi ribbons was most beneficial for optimizing the interfacial bond strength between NiTi SMA and carbon fiber-reinforced epoxy composites when bonded with the Hysol® 9696U (Henkel Corporation) film adhesive. Double lap shear data revealed that interfacial bond strength between NiTi and PMCs were approximately 20 percent higher for primed NiTi than that of the NiTi-PMC without primer. Optical micrographs also supported the double lap shear data, which suggested that Hysol® 9696U did not adhere as well to NiTi surfaces without primer compared to the NiTi with a primer.

The Hysol® 9696U adhesive exhibited the highest and most consistent adhesive joint strength between primed NiTi and PMCs among all three adhesive candidates studied. Further analysis of the failure modes by optical microscopy revealed that Hysol® 9696U exhibited mostly cohesive failure through the adhesive layer, which is the desirable failure mode for adhesive-bonded materials. Determining the most ideal adhesive for NiTi–PMC with one type of primer was the focus of this study, but investigating other primers and bond strength durability are other concerns that should be addressed to aid in determining the feasibility of implementing an adhesive-bonded SMA-PMC adaptive structure.

Additional experiments evaluating the damping performance of NiTi-PMC hybrid specimens using Hysol® 9696U film adhesive as a function of NiTi surface treatment were investigated using dynamic mechanical analysis (DMA). DMA data revealed multiple transitions in the storage modulus (E'), loss modulus (E''), and damping factor (tan δ) data in all NiTi-PMC samples, which arose from the NiTi phase transformations and the glass-transition temperatures (T_g's) of the film adhesive and PMC matrix. The most noticeable changes from DMA regarding damping were detected from the loss modulus data, which in some instances varied considerably in the surface-treated NiTi-PMC hybrid specimens compared to the untreated specimens.

The tan δ for the PMC alone was the highest compared to those of the NiTi-PMC materials at room temperature. This behavior would typically suggest that NiTi-PMC samples were more elastic (stiffer) than the PMCs. In this study, the tan δ peak of the PMC was more than likely higher than the NiTi-PMC samples because the relaxation behavior of the epoxy matrix at the T_g was suppressed by the NiTi. Near 100 °C, the tan δ values of the NiTi-PMC laminates were higher than the PMC. Because tan δ also takes into account the relationship between E'' and E', the tan δ data should be analyzed with the data of both the E'' and E' to assess damping capacity.

DMA is often a very useful tool to screen polymers and PMCs for damping and other thermomechanical properties. Because the material introduced to absorb the vibrations was not a polymer, the changes in the tan δ peak maximum and width observed from the NiTi-PMC in the present study may not correspond to the typical thermally induced chain relaxations in polymers; as a result, the tan δ data alone may not truly give an accurate depiction of damping performance in these samples. Future work will involve using a different method to measure the damping performance of NiTi-PMC samples, in addition to tailoring the SMA to enhance its damping response.

References

1. Noor, Ahmed K., et al.: Structures Technology for Future Aerospace Systems. Comput Struct., vol. 74, no. 5, 2000, pp. 507–519.
2. Ott, Eric A.: Shape Changing Airfoil. NASA/CR—2005-213971, 2005. http://ntrs.nasa.gov.
3. Jarali, Chetan S.; Raja, S.; and Upadhya, A.R.: Constitutive Modeling of SMA SMP Multifunctional High Performance Smart Adaptive Shape Memory Composite. Smart Mater. Struct., vol. 19, no. 10, 2010, pp. 105029–105042.
4. Davis, Brian; Turner, Travis L.; and Seelecke, Stefan: Measurement and Prediction of the Thermomechanical Response of Shape Memory Alloy Hybrid Composite Beams. Smart Structures and Materials 2005: Modeling, Signal Processing, and Control, Proceedings of SPIE, R.C. Smith, ed., vol. 5757, paper no. 74, SPIE, Bellingham, WA, 2005.
5. Zheng, Y.J.; Cui, L.S.; and Schrooten, J.: Basic Design Guidelines for SMA/Epoxy Smart Composites. Mater. Sci. Eng., A, vol. 390, nos. 1–2, 2005, pp. 139–143.
6. Turner, Travis L.: Thermomechanical Response of Shape Memory Alloy Hybrid Composites. NASA/TM—2001-210656, 2001. http://ntrs.nasa.gov.
7. Šittner, Petr; Michaud, Veronique; and Schrooten, Jan: Modelling and Material Design of SMA Polymer Composites. Materials Trans., vol. 43, no. 5, 2002, pp. 984–993.
8. de Araújo, C.J., et al.: Fabrication and Static Characterization of Carbon-Fiber-Reinforced Polymers With Embedded NiTi Shape Memory Wire Actuators. Smart Mater. Struct., vol. 17, no. 6, 2008, 065004.

9. Vokoun, D.; Šittner, P.; and Stalmans, R.: Study of the Effect of Curing Treatment in Fabrication of SMA/Polymer Composites on Deformational Behavior of NiTi–5at%Cu SMA Wires. Scripta Mater., vol. 48, no. 5, 2003, pp. 623–627.
10. Antico, F.C., et al.: Adhesion of Nickel-Titanium Shape Memory Alloy Wires to Thermoplastic Materials: Theory and Experiments. Smart Mater. Struct., vol. 21, no. 3, 2012, 035022.
11. Banea, M.D.; and da Silva, L.F.M.: Adhesively Bonded Joints in Composite Materials: An Overview. Proceedings of the Institution of Mechanical Engineers, Part L: Journal of Materials Design and Applications, vol. 223, no. 1, 2009, pp. 1–18.
12. Jonnalgadda, K.; Kline, G.E.; and Sottos, N.R.: Local Displacements and Load Transfer in Shape Memory Alloy Composites. Exp. Mechanics, vol. 37, no. 1, 1997, pp. 78–86.
13. Biao, Qi: Sanding, Grit Blasting and Plasma Etching: Effect on Surface Composition and Surface Energy of Graphite/Epoxy Composites, M.S. Thesis, Univ. of Cincinnati, 2009.
14. Smith, N.A., et al.: Improved Adhesion Between Nickel-Titanium Shape Memory Alloy and a Polymer Matrix Via Silane Coupling Agents. Compos. Part A–Appl. S., vol. 35, no. 11, 2004, pp. 1307–1312.
15. Neuking, K., et al.: Polymer/NiTi-Composites: Fundamental Aspects, Processing and Properties. Adv. Eng. Mater., vol. 7, no. 11, 2005, pp. 1014–1023.
16. Ogisu, Toshimichi, et al.: Damage Behavior Analysis of Smart Composites With Embedded Pre-strained SMA Foils. Smart Mater. Struct., vol. 15, no. 1, 2006, pp. 41–50.
17. Zimmerman, T.J., et al.: Adhesive Bonding of Hybrid Actuated Shape Memory Alloy-Composite Structures. International SAMPE Technical Conference, Salt Lake City, UT, 2010.
18. Zhandarov, Serge; and Mäder, Edith: Characterization of Fiber/Matrix Interface Strength: Applicability of Different Tests, Approaches and Parameters. Compos. Sci. Technol., vol. 65, no. 1, 2005, pp. 149–160.
19. Poon, Chi-kin, et al.: Interfacial Debond of Shape Memory Alloy Composites. Smart Mater. Struct., vol. 14, 2005, pp. N29–N37.
20. Dawood, M.; El-Tahan, M.W.; and Zheng, B.: Bond Behavior of Superelastic Shape Memory Alloys to Carbon Fiber Reinforced Polymer Composites. Compos. Part B–Eng., vol. 77, 2015, pp. 238–247.
21. Poon, Chi-kin; Lau, Kin-tak; and Zhou, Li-min: Design of Pull-Out Stresses for Prestrained SMA Wire/Polymer Hybrid Composites. Compos. Part B–Eng., vol. 36, no. 1, 2005, pp. 25–31.
22. Min, J.B., et al.: Adhesive-Bonded Shape Memory Alloy Strip Joint for Composite Fan Blade Shape Changing Concept. AIAA 2016–1501, 2016.
23. Kinloch, Anthony: Adhesion and Adhesives: Science and Technology, Chapman and Hall Ltd., London, UK, 1987.
24. Hexcel Composites: Hexply 8552 Material Safety Data Sheet. April 1, 2009. https://shedapps.grc.nasa.gov/pdf/MSDS2010/grc-5038a-462.pdf Accessed June 15, 2018.
25. ASTM D3528–96: Standard Test Method for Strength Properties of Double Lap Shear Adhesive Joints by Tension Loading. ASTM International, West Conshohocken, PA, 2016.
26. Schmidt, Ina; and Lammering, Rolf: The Damping Behavior of Superelastic NiTi Components. Mater. Sci. Eng., A, vol. 378, nos. 1–2, 2004, pp. 70–75.